X-shaped Radical Offshore Wind Turbine for Overall Cost of Energy Reduction

D3.3

Control model of X-ROTOR

https://xrotor-project.eu

@XROTORProject

June 2022

This project has received funding from the European Union's Horizon 2020 research and innovation programme under grant agreement No 101007135

Ref. Ares(2022)4807484 - 30/06/2022

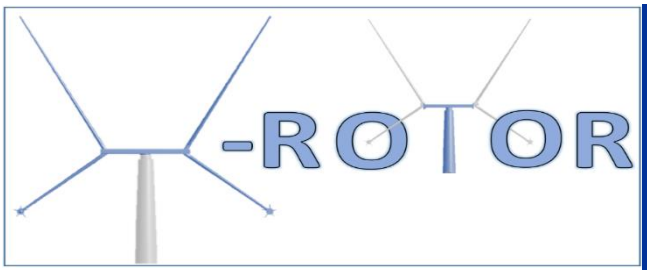

X-SHAPED RADICAL OFFSHORE WIND TURBINE FOR OVERALL COST OF ENERGY REDUCTION

Project acronym: **XROTOR**
Grant agreement number: 101007135
Start date: 01st January 2021
Duration: 3 years

WP3 X-Rotor Control
T3.3 – Control Design Models of X-Rotor Concept
D3.3 Control Model of X-Rotor

Lead Beneficiary: University of Strathclyde

Delivery date: 30/06/2022

Author(s) information (alphabetical):		
Name	Organisation	Email
William Leithead	University of Strathclyde	w.leithead@strath.ac.uk
Laurence Morgan	University of Strathclyde	Laurence.morgan@strath.ac.uk
Adam Stock	University of Strathclyde	Adam.stock@strath.ac.uk

Document Information

Version	Date	Description	Prepared by	Reviewed by	Approved by
1	30/06/2022	Version 1	William Leithead	James Carroll	James Carroll

The XROTOR Project has received funding from the European Union's Horizon 2020 research and innovation programme under grant agreement no. 101007135.

Executive Summary

Deliverable Description:

This deliverable report supports deliverable D3.3 *"Control Design Models of X-Rotor Concept"*, and details the design and development of a set of linear control design models for the X-Rotor concept, which aim to provide a transparent tool for controller design.

Responsible:

The responsible partner is the University of Strathclyde, with Prof. W.E. Leithead as the principle investigator.

Outcome Summary:

The X-Rotor concept consists of a large vertical axis primary rotor with smaller secondary horizontal axis rotors mounted on the primary rotor to extract power. Both the pitch angle of the primary rotor blades and the thrust of the secondary rotors can be adjusted to control the turbine.

Based on the work being undertake in Tasks 3.1 and 3.4, it is clear, that the inputs to the X-rotor full envelop controller are the primary rotor speed and secondary rotor speeds or equivalently the frequencies of the power connections to the generators. The outputs are pitch angle demand for the upper primary rotor blades and a parameter that is equivalent to a tip speed ratio demand. It is, also clear that a separate controller incorporated into each power take-off unit, consisting of a secondary rotor, generator and converter, is required. These additional controllers are tasked with ensuring that the secondary rotor speed and aerodynamic torque maintain the relationship required to achieve the required tip speed ratio.

A nonlinear dynamic model of the power take-off unit and its associated linearised model, suitable for design of the power take-off controller are described. In addition, a nonlinear dynamic model of the X-rotor turbine and its associated linearised model, suitable for design of the full envelop controller, are described. A MATLAB script to determine the linear models for a given X-rotor operational strategy is developed and some illustrative examples provided.

Contents

Executive Summary i
1 Introduction 2
2 Overview of operational strategy and controller structure 3
3 Power take-off system controller design model 6
3.1 Power take-off unit nonlinear model 6
3.2 Power take-off unit linear model 7
4 Full envelop controller design model 9
4.1 Nonlinear model for full envelop controller design 9
4.2 Linear model for full envelop controller design 10
5 Illustrative exaples of the linear dynamics 13
6 Conclusions 14
7 References 15

1 Introduction

The X-Rotor concept is an innovative wind turbine design that consists of a large vertical axis primary rotor with smaller secondary horizontal axis rotors mounted on it to extract power. The pitch angle of the primary rotor blades can be altered to control the aerodynamic torque and the thrust of the secondary rotors can also be controlled. A visualisation of the concept is shown in Figure *1*.

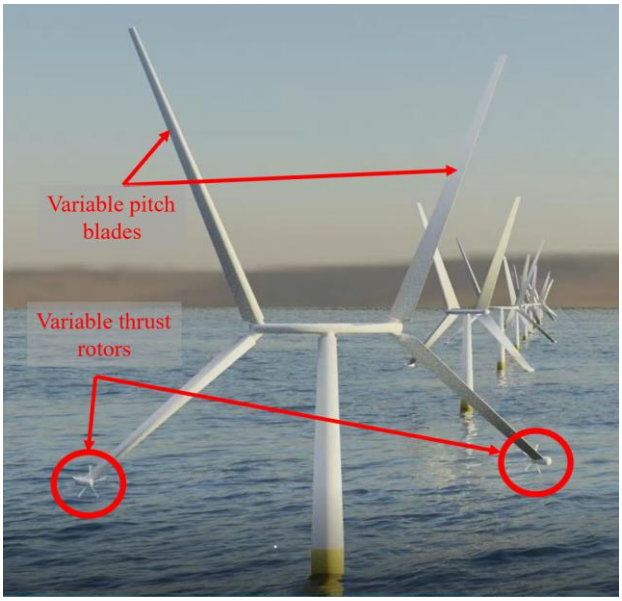

Figure 1: X-Rotor concept

In prior deliverable D3.2 [4], a control simulation model was created for the X-Rotor concept that models the necessary fundamental dynamics and allows controllers for the turbine to be tested. To design the controllers, linearised models of a system are required for linear control analysis and design. The controllers can then be applied to the aforementioned control simulation model (which is highly non-linear) to ensure that transient conditions are suitably dealt with and to quantify the controller performance.

Any controller must follow a control strategy, i.e. the controller aims to ensure the turbine tracks given operating points at given wind speeds using available control signals. The control strategy directly impacts both the power capture and the structural loads experienced by the turbine. The choice of control strategy, also, impacts on the nature of the control design models. It is therefore essential to review the control strategy prior to the development of the control design models for the X-Rotor.

In this report, the creation of suitable linearised control models is detailed. In Section 2, an overview of the X-Rotor's operational strategy and the structure of the dynamics of the turbine and its controller is given. In Section 3, a nonlinear model and an associated linear model of the power take-off system dynamics, suitable for its controller design, are presented. In Section 4, a nonlinear model and an associated linear model of the X-Rotor turbine dynamics, suitable for its full envelop controller design, are presented. In Section 5, some illustrative examples of the linear dynamics are provided and, in Section 6, conclusions are drawn.

2 Overview of operational strategy and controller structure

The specification of the operational strategy for the X-Rotor is being investigated in Task 3.1 and the controller to realise the operational strategy is being designed in Task 3.4. Although completion of these tasks is not due till months 34 and 33, respectively, it is already clear that the operational strategy consists of several different modes.

Mode 1 – Constant secondary rotor speed: In very low wind speeds, just above cut-in, the average secondary rotor speed is held constant with the tip speed ratio for each rotor independently varying with wind speed. (When considering the X-Rotor turbine's operational strategy, since the strategy is defined by the equilibrium operating points for each wind speed, the average rotor speed would is defined as the average over one rotation of the primary rotor. However, for any practical controller dependent on average rotor speed, this definition is not appropriate due to the time-varying nature of the wind speed. Instead in practical controllers, since the variation of the rotor speed during a rotation is dominated by a sinusoid, the average the two rotor speeds of the two secondary speeds is preferred. In this way, a time-varying estimate of rotor speed is obtained.) Suppose each power take-off unit, i.e. secondary rotor, generator and associated power converter, is operated such that $Q_S = k_c\Omega_S^2$ or equivalently $T_e = k_c(\omega_e/p)^2$, where Q_S is the secondary rotor's aerodynamic torque, Ω_s is its rotational speed, T_e is generator reaction torque, ω_e is the frequency of the AC connection to the generator and p is the number of generator pole pairs. For each value of k_c, the secondary rotor operates at some specific tip speed ratio. Hence, by varying k_c, the tip speed ratio for the secondary rotor can be varied as required. It follows that the average secondary rotor speed can be maintained at a fixed value by the feedback loop in Figure 1, where Ω_{S1} and Ω_{S2} are the rotor speeds of the two secondary rotors and $\overline{\Omega}_{SR}$ is the required average secondary rotor speed.

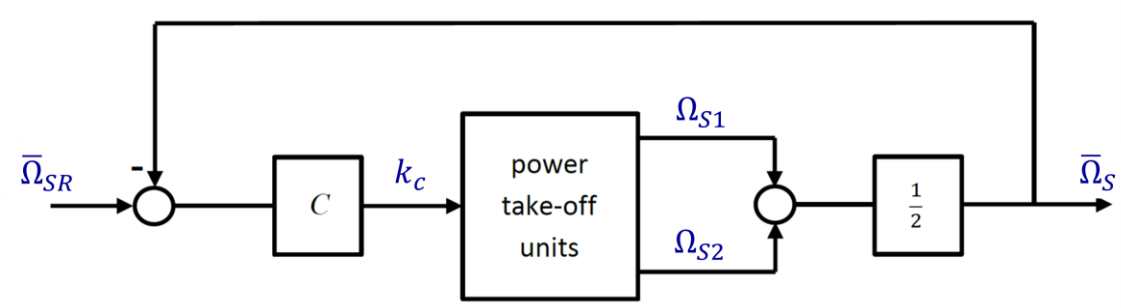

Figure 1: Constant secondary rotor speed control

A commonly used device to present operational strategies for HAWTs is the torque/speed diagram, whereon the locus of equilibrium operating points is plotted on the rotor torque/rotor speed plane. The corresponding device for the X-Rotor concept is the combination primary rotor torque/speed diagram and secondary rotor thrust/speed diagram, whereon the locus of equilibrium operating points is plotted on the secondary rotor thrust/rotor speed plane see Figure 2. In the latter, thrust is scaled by the primary rotor diameter so that primary and secondary rotor equilibrium operating points lie on horizontal lines. Mode 1 is plotted on Figure 2.

Mode 2 – C_{Pmax} tracking: In intermediate wind speeds, energy capture is maximised. Since the relationships between secondary rotor torque and secondary rotor speed, secondary rotor thrust and secondary rotor speed, and primary rotor torque and primary rotor speed are all quadratic, both the primary and secondary rotors can be caused to operate at their aerodynamic coefficients' maximum value through an appropriate choice for the value of k_c, say k_{opt}; that is, $k_c = k_{opt}$. Mode 2 is plotted on the combined primary rotor torque/speed and secondary rotor thrust/speed diagrams in Figure 3.

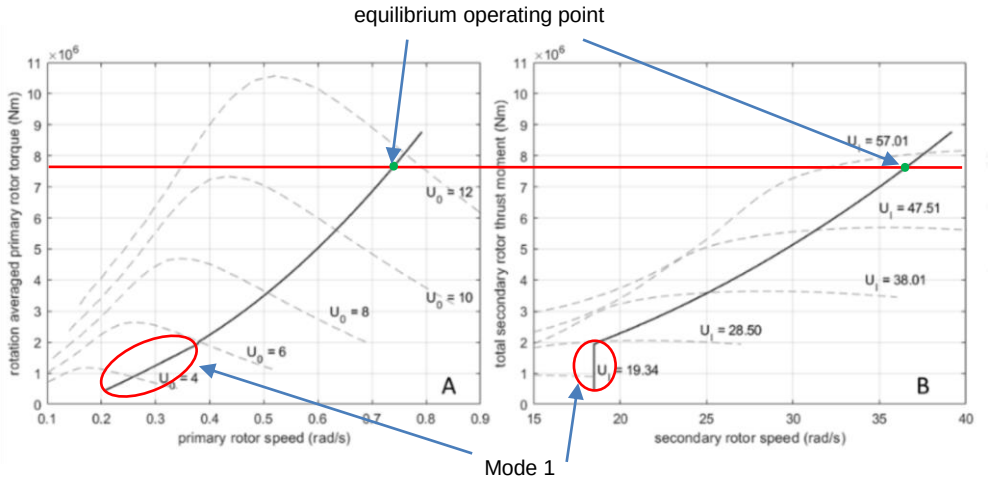

Figure 2: Operating strategy Mode 1

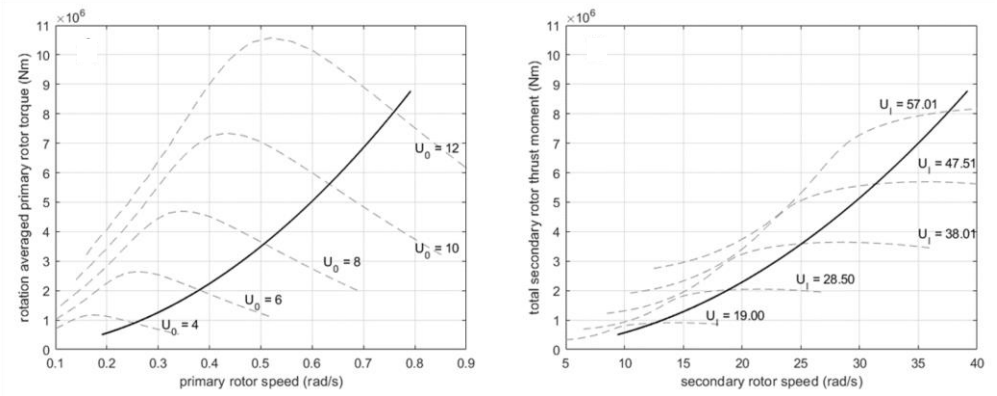

Figure 3: Operating strategy Mode 2

Mode 3 – pre-emptive pitching: In wind speeds just below rated wind speed, the upper blades on the primary rotor can be pitched to reduce pitch activity that otherwise would be very high in wind speeds just above rated. As the primary rotor speed continues to increase in these wind speeds, the blade pitch angle, β_d, can be adjusted as a function of primary rotor speed, Ω_P; that is, $\beta_d = f(\Omega_P)$, for some appropriate choice of the function, $f(\cdot)$. The introduction of this pitch adjustment in below rated wind speed displaces the operating state of the primary rotor from C_{Pmax} tracking, thereby reducing the primary rotor torque. The secondary rotor thrust must be reduced by a matching reduction in the secondary rotor thrust. To do so, as the average secondary rotor speed continues to increase in these wind speeds, k_c is adjusted as a function of $\overline{\Omega}_S = \frac{1}{2}(\Omega_{S_1} + \Omega_{S_2})$; that is, $k_c = g(\overline{\Omega}_S)$, for some appropriate choice of the function, $g(\cdot)$. Mode 3, with pitch increasing linearly between 11.5m/s and 12.5m/s, is plotted on the combined primary rotor torque/speed and secondary rotor thrust/speed diagrams in Figure 4.

Mode 4 – Constant torque and rotor speed: In above rated wind speed, the average thrust from the secondary rotors is held constant through an appropriate choice for the value of k_c, say k_a; that is, $k_c = k_a$. the primary rotor speed is held constant by adjusting the angle of pitch of the upper blades of the primary rotor.

It is clear from the above discussion that the full envelope controller for the X-Rotor concept acts through adjusting k_c and β_d in response to measurements of Ω_P and Ω_s or ω_e. A schematic diagram for the interplay between the dynamics of the turbine full envelop controller and the dynamics of the primary rotor and the power take-off system is depicted in Figure 5. Only the main inputs and outputs to the

power take-off unit are included. For simplicity of interpretation only one power take-off system is explicitly represented.

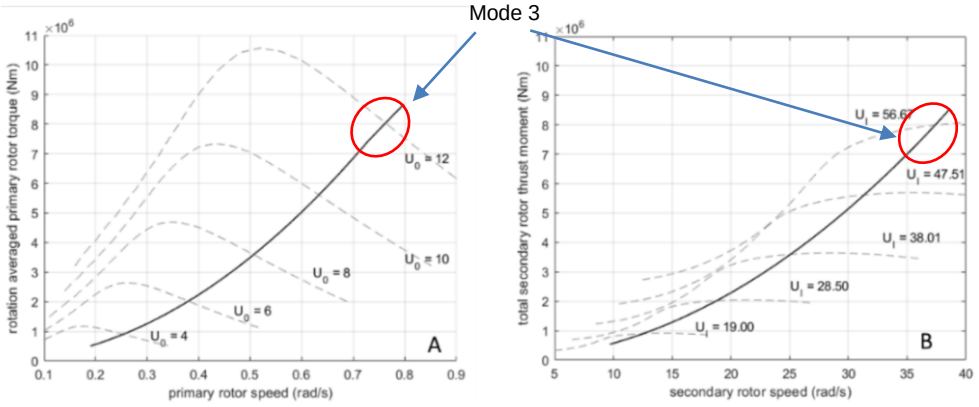

Figure 4: Operating strategy mode 3

It is, also, clear that the X-Rotor has two controllers, a full envelop controller that regulates the operation of the primary rotor to deliver the operational strategy and a controller that regulates the power take-off system to ensure $Q_S = k_c\Omega_S^2$ or equivalently $T_e = k_c(\omega_e/p)^2$. For each of these controllers a suitable linearised model is required for controller design purposes.

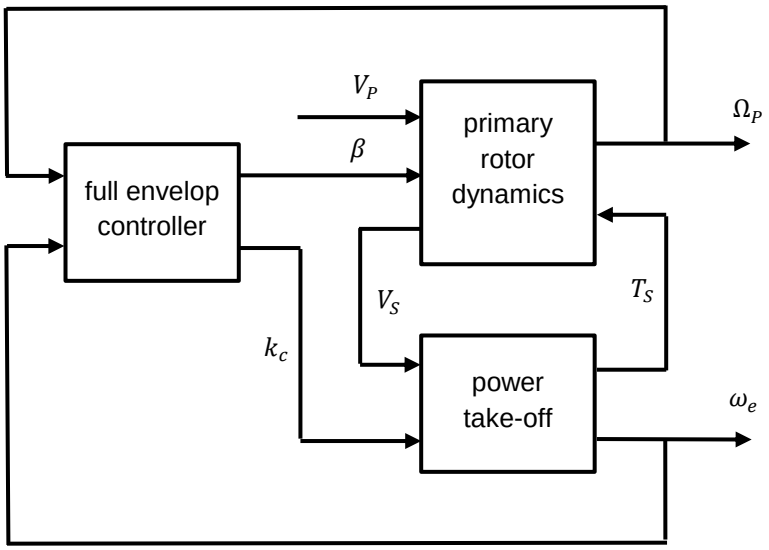

Figure 5: Dynamic structure of turbine and controller

3 Power take-off system controller design model

As represented in Figure 6, the power take-off system has one exogenous input, V_S, the wind speed as experienced by the secondary rotor, and one control input, k_c, for regulating the tip speed ratio. It has one output regulating the primary rotor, namely, secondary rotor thrust, T_S. Three auxiliary variables are determined by the model of the power take-off dynamics, the secondary rotor torque, Q_S, rotor speed, Ω_S, and tip speed ratio, λ_S.

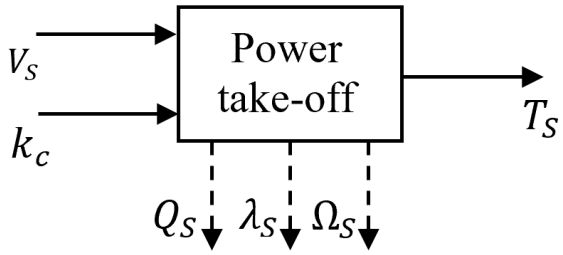

Figure 6: Non-linear model of the power take-off by secondary rotors

A schematic diagram for the power take-off system is shown in Figure 7.

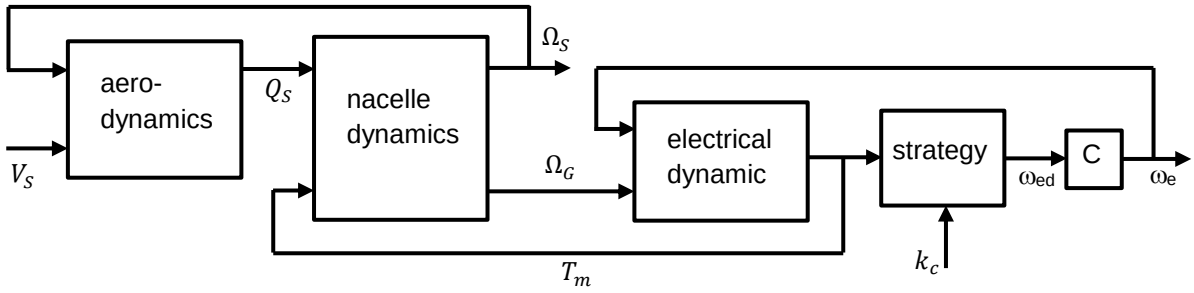

Figure 7: Power take-off schematic diagram

The power take-off system includes a controller, represented by *strategy* together with C. (Italicised text is used to indicate when sub-systems in Figure 7 are being referred to.)

As well as ensuring $Q_S = k_c\Omega_S^2$ or equivalently $T_e = k_c(\omega_e/p)^2$, the objectives for this controller are to ensure the power take-off system is adequately damped and to maintain the secondary rotor at a specified tip speed ratio.

3.1 Power take-off unit nonlinear model

The *aerodynamics* for the secondary rotors is modelled by the standard relationships for torque and thrust, namely,

$$Q_S(\Omega_S, V_S) = \tfrac{1}{2}\rho A_S R_S V_S^2 C_{QS}(\lambda_S) \quad ; \quad T_S(\Omega_S, V_S) = \tfrac{1}{2}\rho A_S V_S^2 C_{TS}(\lambda_S) \quad ; \quad \lambda_S = R_S\Omega_S/V_S \tag{1}$$

where ρ is the density of air, A_S is the secondary rotor area, R_S is its radius and C_{QS} and C_{TS} are its aerodynamic torque and thrust coefficients, respectively.

The *nacelle dynamics* are modelled by a 2 lumped-inertia system

$$J_S\dot{\Omega}_S = Q_S - T_{RG} \quad ; \quad \dot{T}_{RG} = K_S(\Omega_S - \Omega_G) \quad ; \quad J_G\dot{\Omega}_G = T_{RG} - T_m \tag{2}$$

where inertia, J_S, is dominated by the inertia of the secondary rotor, the inertia, J_G, is the combined inertia of the rotor hub and generator rotor, K_S is the stiffness of the secondary rotor, T_{RG} is the in-plane

blade bending torque, Ω_G is the generator speed and T_m is the generator reaction torque. Due to the power take-off being direct drive, viscous damping losses are negligible and are omitted. Even taking into account aerodynamic damping, the nacelle dynamics are a lightly damped second order system with frequency related to the rotor symmetric mode frequency.

The nacelle dynamics together with the generator electrical system is equivalent to the standard swing equation for a generator [1]**.** The generated power is proportional to the phase difference between the mechanical frequency and the electrical frequency, that is, it is proportional to the integral of $(p\Omega_G - \omega_e)$, where ω_e is electrical frequency and p is the number of pole pairs. It is assumed that the power electronics and their internal controllers are configured such that *electrical dynamics*, consisting of generator electrical system, power electronics and their internal controllers, are dynamically equivalent to the system

$$\dot{T}_e = k_e(\Omega_G - \omega_e/p) \quad ; \quad T_m = T_e/E_{ff} \tag{3}$$

over a frequency range greater than the bandwidth of nacelle dynamics and the bandwidth of the transmittance from k_c to Ω_S, where T_e is electrical torque and E_{ff} is combined efficiency of generator and power electronics; that is, it behaves similarly to an induction generator [1]

The relationship between aerodynamic torque and generator frequency, corresponding to a specified secondary rotor tip speed ratio, is defined in *strategy* such that

$$\tilde{\omega} = p\sqrt{\hat{Q}_A/k_c} \quad ; \quad \dot{\omega}_{ed} = a(\tilde{\omega} - \omega_{ed}) \tag{4}$$

where k_c is the control input for setting the tip speed ratio and $\hat{Q}_A$ is an estimate of aerodynamic torque. The simplest choice would be $\hat{Q}_A = T_m$. Due to the low inertia of the secondary rotor, it might be expected that the power take-off system would be sufficiently responsive to cater for the changes in wind speed with azimuthal angle. If this is not the case, a better choice of aerodynamic torque of the form, $\hat{Q}_A = h_1(s)T_m + h_2(s)\Omega_G$ [2] would be required. The rate of change of demanded electrical frequency, induced by changes in k_c, must be kept comfortably within limits acceptable to the power electronics. This could be achieved through inclusion of a rate limited low pass filter in C. However, here the low pass filter is included within *strategy* to highlight its importance.

In constant speed HAWTs, induction generators provide sufficient damping that the drive-train is not resonant. However, that may not be the case for the secondary rotors. Accordingly, C could include an inner feedback loop to damp the nacelle dynamics. This inner feedback loop is not shown in the above diagram. In addition, C includes an outer feedback loop to ensure that λ_S tracks the secondary rotor operating strategy, irrespective of azimuthal angle of the primary rotor. This inner/outer feedback loop structure is similar to PSS/AVRs in electrical generators [3] or to drive-train filters in variable speed pitch regulated HAWTs, whereby, an inner feedback loop acting through generator reaction torque is used to increase damping of the first drive train mode and an outer feedback loop is used to regulated rotor speed. In both these examples, the inner feedback loop is active over a narrow band of frequencies greater than the bandwidth of outer feedback loop.

3.2 Power take-off unit linear model

An equilibrium operating point for the power take-off can be specified by the value of tip speed ratio, λ_{S0}, and the secondary rotor speed averaged over a single rotation of the primary rotor, Ω_{S0}. The pairs, $(\lambda_{S0}, \Omega_{S0})$, are determined by the X- Rotor turbine's operating strategy. The corresponding equilibrium values for all other variables are then obtained from the nonlinear model with all rates of change set to zero.

The linear dynamics relative to the equilibrium operating point

$$(\lambda_{S0}, \Omega_{S0}; Q_{S0}, V_{S0}, \Omega_{S0}, T_{S0}, T_{RG0}, \Omega_{G0}, T_{m0}, T_{e0}, \omega_{e0}, \hat{Q}_A, \tilde{\omega}_0, \omega_{ed0}) \tag{5}$$

are

$$\Delta Q_S = \frac{\partial Q_S}{\partial \Omega_S}\Delta\Omega_S + \frac{\partial Q_S}{\partial V_S}\Delta V_S \quad ; \quad \Delta T_S = \frac{\partial T_S}{\partial \Omega_S}\Delta\Omega_S + \frac{\partial T_S}{\partial V_S}\Delta V_S \tag{6}$$

$$\Delta Q_S = \frac{\partial Q_S}{\partial \Omega_S}\Delta\Omega_S + \frac{\partial Q_S}{\partial V_S}\Delta V_S \quad ; \quad \Delta T_S = \frac{\partial T_S}{\partial \Omega_S}\Delta\Omega_S + \frac{\partial T_S}{\partial V_S}\Delta V_S \tag{7}$$

$$J_S\Delta\dot{\Omega}_S = \Delta Q_S - \Delta T_{RG} \quad ; \quad \Delta\dot{T}_{RG} = K_S(\Delta\Omega_S - \Delta\Omega_G) \quad ; \quad J_G\Delta\dot{\Omega}_G = \Delta T_{RG} - \Delta T_m \tag{8}$$

$$\Delta\dot{T}_e = k_e(\Delta\Omega_G - \Delta\omega_e/p) \quad ; \quad \Delta T_m = \Delta T_e/E_{ff} \tag{9}$$

$$\Delta\hat{Q}_A = h_1(s)\Delta T_m + h_2(s)\Delta\Omega_G \quad ; \quad \Delta\tilde{\omega} = \frac{\partial\tilde{\omega}}{\partial\hat{Q}_A}\Delta\hat{Q}_A + \frac{\partial\tilde{\omega}}{\partial k_c}\Delta k_c \quad ; \quad \Delta\dot{\omega}_{ed} = a(\Delta\tilde{\omega} - \Delta\omega_{ed}) \tag{10}$$

These linear dynamics can be used to design the controller, C.

4 Full envelop controller design model

The structure of the full envelop controller and turbine is shown in Figure 5. The X-Rotor control simulation model [4] is simplified in the following manner:

- The variation of aerodynamic torques and moments with azimuthal angle is neglected; that is, the aerodynamic coefficients are averaged over azimuthal angle.
- The cross-arm is considered rigid.
- The lower blades are considered rigid. (From [5] and simulations using the Control Simulation Model [4], it is clear that the flexing of the lower blades are very much stiffer and flex much less than the upper blades.)
- The upper blades are represented by a “single blade model” whereby only the lowest tangential and normal dynamic modes, with tangential displacement and normal displacement for each blade the same, are included.
- The pitch angle for both blades are the same.

On the premise that the specification of the pitch actuator and so its dynamics is determined from the control design task, the pitch actuator dynamics are included in the full envelope controller rather than in the primary rotor dynamics.

4.1 Nonlinear model for full envelop controller design

The simplified dynamics for the upper rotor are

$$J_P\begin{bmatrix}\dot{\Omega}_P\\ \dot{\Phi}_P\end{bmatrix} = -J_P\begin{bmatrix}\left(\omega_e^2 c_\beta^2 + \omega_f^2 s_\beta^2\right) & -\left(\omega_e^2 - \omega_f^2\right)s_\beta c_\beta\\ -\left(\omega_e^2 - \omega_f^2\right)s_\beta c_\beta & \left(\omega_e^2 s_\beta^2 + \omega_f^2 c_\beta^2\right)\end{bmatrix}\begin{bmatrix}\theta_P - \theta_H\\ \phi_P - \psi\end{bmatrix}$$

$$-J_P\begin{bmatrix}\left(\gamma_e c_\beta^2 + \gamma_f s_\beta^2\right) & -\left(\gamma_e - \gamma_f\right)s_\beta c_\beta\\ -\left(\gamma_e - \gamma_f\right)s_\beta c_\beta & \left(\gamma_e s_\beta^2 + \gamma_f c_\beta^2\right)\end{bmatrix}\begin{bmatrix}\Omega_P - \dot{\theta}_H\\ \Phi_P\end{bmatrix} + \begin{bmatrix}M_{PA\theta}(V_P, \Omega_P, \beta)\\ M_{PA\phi}(V_P, \Omega_P, \beta)\end{bmatrix} \tag{11}$$

$$+\begin{bmatrix}0\\ \left(J_P + \tilde{J}_P\right)\Omega_P^2\cos(\phi_P) + gM_P\ell_{Pcm}\sin(\phi_P)\end{bmatrix}$$

and

$$\begin{bmatrix}\dot{\theta}_P\\ \dot{\phi}_P\end{bmatrix} = \begin{bmatrix}\Omega_P\\ \Phi_P\end{bmatrix} \tag{12}$$

where θ_P and ϕ_P are, respectively, the tangential and normal angular displacement of the upper blades, θ_H is the angular dispacement of the cross-arm, ψ is the coning angle of the upper blade, β is the pitch angle of the upper blades, ω_e and ω_f are , respectively, the tangential and normal frequencies of the upper blades, γ_e and γ_f are, respectively, tangential and normal damping coefficients of the upper blades, J_P is the inertia of the upper blades, $M_{PA\theta}$ and $M_{PA\phi}$ are, respectively, the tangential and normal aerodynamic blade bending moments for the upper blades, g is the gravity, M_P is the mass of the upper blades, ℓ_{Pcm} is the distance between the upper blade centre of gravity and its root and R_P is the radius of the upper rotor. In addition,

$$\omega_e^2 = K_e/J_P \quad ; \quad \omega_f^2 = K_f/J_P \quad ; \quad \tilde{J}_P = M_P\left(\ell_c^2 + 2\ell_c\ell_{Pcm}\sin(\phi_P) - \ell_c^2\sin^2(\phi_P)\right) \tag{13}$$

where K_e and K_f are, respectively, the tangential and normal upper blade stiffnesses and ℓ_c is the radius of the cross-arm. (The parameter values for one blade can be used here without changing these dynamics.)

The torque acting on on the cross-arm due to the upper primary rotor is

$$Q_{PU} = J_P\omega_e^2\big[(\theta_P - \theta_H)c_\beta - (\phi_P - \psi)s_\beta\big]c_\beta + J_P\omega_f^2\big[(\theta_P - \theta_H)s_\beta - (\phi_P - \psi)c_\beta\big]s_\beta \qquad (14)$$

$$+J_P\big[(\gamma_e c_\beta^2 + \gamma_f s_\beta^2)(\Omega_P - \dot{\theta}_H) - (\gamma_e - \gamma_f)s_\beta c_\beta \phi_P$$

and the dynamics for the cross-arm and lower blades are,

$$J_H\dot{\Omega}_H = Q_{PU} + Q_{PL} - R_P T_S \quad ; \quad \dot{\theta}_H = \Omega_H \qquad (15)$$

where J_H is the combined inertia of the cross-arm, lower blades and power take-off, Q_{PL} is the aerodynamic torque from the (assumed stiff) lower primary rotor blades and T_S is the thrust from the secondary rotors. (When parameter values for one blade are used in Q_{PU} and Q_{PL}, T_S is the thrust on one secondary rotor and J_H is half the inertia of the combined inertia.)

The *power take-off* is treated as an actuator. It is simplified in the following manner:

- The azimuthal variation in wind speed experienced by the secondary rotor is neglected.
- The azimuthal variation in wind speed experienced by the secondary rotor is neglected.
- C, the controller embedded in the power take-off, is chosen to be fast acting relative to the full envelope controller.
- The electrical dynamics are at relatively high frequency.

Since the azimuthal variation in wind speed is being neglected, the response of the power take-off can be slower and the simplest choice of aerodynamic torque estimator suffices; that is, $\hat{Q}_A = T_m$. The resulting dynamics for the power take-off are

$$Q_S(\Omega_S, \Omega_P) = \tfrac{1}{2}\rho A_S R_S V_S^2(1 + 0.5\lambda_S^{-2})C_{QS}(\lambda_S) \quad ; \quad T_S(\Omega_S, \Omega_P) = \tfrac{1}{2}\rho A_S V_S^2(1 + 0.5\lambda_S^{-2})C_{TS}(\lambda_S) \qquad (16)$$

$$\lambda_S = R_S\Omega_S/V_S \quad ; \quad V_S = R_P\Omega_P \qquad (17)$$

$$J_S\dot{\Omega}_S = Q_S - T_{RG} \quad ; \quad \dot{T}_{RG} = K_S(\Omega_S - \Omega_G) \quad ; \quad J_G\dot{\Omega}_G = T_{RG} - k_c\Omega_G^2 \qquad (18)$$

At a constant tip speed ratio, the secondary rotors experience a wind speed that includes a strong sinusoidal variation in azimuthal angle due to their rotation into and out of the ambient wind acting on the X-Rotor turbine. Averaged over azimuthal angle, this variation in wind speed increases the aerodynamic thrust and torque by a factor, $(1 + 0.5\lambda_P^{-2})$ [5]. Hence, its inclusion in the expression for T_S.

Furthermore, when the bandwidth of the power take-off is sufficiently large, it can be assumed that $Q_S = k_c\Omega_S^2$. The dynamics simply further to

$$Q_S(\Omega_P, k_c) = \tfrac{1}{2}\rho A_S R_S V_S^2(1 + 0.5\lambda_P^{-2})C_{QS}(\lambda_S) \quad ; \quad T_S(\Omega_P, k_c) = \tfrac{1}{2}\rho A_S V_S^2(1 + 0.5\lambda_P^{-2})C_{TS}(\lambda_S) \qquad (19)$$

$$\lambda_S = h(k_c) \quad ; \quad V_S = R_P\Omega_P \qquad (20)$$

where λ_S is the solution $k_c\lambda_S^2 = \tfrac{1}{2}\rho A_S R_S^3(1 + 0.5\lambda_P^{-2})C_{QS}(\lambda_S)$.

No aspect of the above nonlinear model for the X-Rotor retains any dependence on azimuthal angle. Furthermore, this dynamic model is quite similar to the control design model for a HAWT [6], albeit with the tower and drive-train dynamics omitted and a rather unusual reaction torque actuator. Accordingly, the nonlinear model for the X-Rotor can be linearised in the usual manner [6].

4.2 Linear model for full envelop controller design

An equilibrium operating point for the power take-off can be specified by the value of wind speed, V_{P0}, pitch angle, β_0, control demand, k_{c0}, and the induced wind speed, V_{S0}. The quadruples, $(V_{P0}, \beta_0, k_{c0}, V_S)$, are determined by the X-Rotor turbine's operating strategy. The corresponding equilibrium values for

all other variables are then obtained from the nonlinear model with all rates of change set to zero. Prior to linearising the dynamics, the following transformation of variables is made:

$$\Omega_P \longrightarrow \Omega_{H0} + \Delta\Omega_P \quad ; \quad \theta_P \longrightarrow \Omega_{H0}t + \Delta\theta_P \quad ; \quad \Omega_H \longrightarrow \Omega_{H0} + \Delta\Omega_H \quad ; \quad \theta_H \longrightarrow \Omega_{H0}t + \Delta\theta_H \tag{21}$$

The equilibrium operating points for θ_P and θ_H are now well defined. The only term in the dynamics explicitly changed by this transformation is Ω_P^2 in the upper blade dynamics which becomes $(\Omega_{H0} + \Delta\Omega_P)^2$.

Relative to the equilibrium operating point

$$(V_{P0}, \beta_0, k_{c0}, V_{S0}; \Omega_{H0}, \theta_{P0}, \theta_{H0}, \phi_{P0}, \Omega_{P0}, \Phi_{P0}, M_{PA\theta 0}, M_{PA\phi 0}, T_{S0}, \Omega_{G0}, T_{RG0}, \lambda_{S0}) \tag{22}$$

the linear dynamics for the upper rotor are

$$J_P \begin{bmatrix} \Delta\dot{\Omega}_P \\ \Delta\dot{\Phi}_P \end{bmatrix} = -J_P \begin{bmatrix} (\omega_e^2 c_{\beta_0}^2 + \omega_f^2 s_{\beta_0}^2) & -(\omega_e^2 - \omega_f^2) s_{\beta_0} c_{\beta_0} \\ -(\omega_e^2 - \omega_f^2) s_{\beta_0} c_{\beta_0} & (\omega_e^2 s_{\beta_0}^2 + \omega_f^2 c_{\beta_0}^2) \end{bmatrix} \begin{bmatrix} \Delta\theta_P - \Delta\theta_H \\ \Delta\phi_P \end{bmatrix}$$

$$-J_P \begin{bmatrix} (\gamma_e c_{\beta_0}^2 + \gamma_f s_{\beta_0}^2) & -(\gamma_e - \gamma_f) s_{\beta_0} c_{\beta_0} \\ -(\gamma_e - \gamma_f) s_{\beta_0} c_{\beta_0} & (\gamma_e s_{\beta_0}^2 + \gamma_f c_{\beta_0}^2) \end{bmatrix} \begin{bmatrix} \Delta\Omega_P - \Delta\Omega_H \\ \Delta\Phi_P \end{bmatrix}$$

$$-J_P \begin{bmatrix} -\sin(2\beta_0) & -\cos(2\beta_0) \\ -\cos(2\beta_0) & \sin(2\beta_0) \end{bmatrix} \left\{ (\omega_e^2 - \omega_f^2) \begin{bmatrix} \theta_{P0} - \theta_{H0} \\ \phi_{P0} - \psi \end{bmatrix} + (\gamma_e - \gamma_f) \begin{bmatrix} \Omega_{P0} - \Omega_{H0} \\ \Phi_{P0} \end{bmatrix} \right\} \Delta\beta \tag{23}$$

$$+ \begin{bmatrix} \frac{\partial M_{PA\theta}}{\partial \Omega_P} \\ \frac{\partial M_{PA\phi}}{\partial \Omega_P} \end{bmatrix} \Delta\Omega_P + \begin{bmatrix} \frac{\partial M_{PA\theta}}{\partial \beta} \\ \frac{\partial M_{PA\phi}}{\partial \beta} \end{bmatrix} \Delta\beta + \begin{bmatrix} \frac{\partial M_{PA\theta}}{\partial V_P} \\ \frac{\partial M_{PA\phi}}{\partial V_P} \end{bmatrix} \Delta V_P$$

$$+ \begin{bmatrix} 0 \\ -(J_P + \tilde{J}_P)\Omega_{H0}^2 \sin(\phi_{P0}) + g M_P \ell_{Pcm} \cos(\phi_{P0}) \end{bmatrix} \Delta\phi_P + \begin{bmatrix} 0 \\ (J_P + \tilde{J}_P) 2\Omega_{H0} \cos(\phi_P)) \end{bmatrix} \Delta\Omega_P$$

and

$$\begin{bmatrix} \Delta\dot{\theta}_P \\ \Delta\dot{\phi}_P \end{bmatrix} = \begin{bmatrix} \Delta\Omega_P \\ \Delta\Phi_P \end{bmatrix} \tag{24}$$

The linear dynamics for the cross-arm are

$$J_H \Delta\dot{\Omega}_H = \Delta Q_P + \Delta Q_{PL} - R_P \Delta T_S \quad ; \quad \Delta\dot{\theta}_H = \Delta\Omega_H \tag{25}$$

$$\Delta Q_P = J_P \begin{bmatrix} (\omega_e^2 c_{\beta_0}^2 + \omega_f^2 s_{\beta_0}^2) & -(\omega_e^2 - \omega_f^2) s_{\beta_0} c_{\beta_0} \end{bmatrix} \begin{bmatrix} \Delta\theta_P - \Delta\theta_H \\ \Delta\phi_P \end{bmatrix}$$

$$+ J_P \begin{bmatrix} (\gamma_e c_{\beta_0}^2 + \gamma_f s_{\beta_0}^2) & -(\gamma_e - \gamma_f) s_{\beta_0} c_{\beta_0} \end{bmatrix} \begin{bmatrix} \Delta\Omega_P - \Delta\Omega_H \\ \Delta\Phi_P \end{bmatrix} \tag{26}$$

$$- J_P \begin{bmatrix} \sin(2\beta_0) & \cos(2\beta_0) \end{bmatrix} \left\{ (\omega_e^2 - \omega_f^2) \begin{bmatrix} \theta_{P0} - \theta_{H0} \\ \phi_{P0} - \psi \end{bmatrix} + (\gamma_e - \gamma_f) \begin{bmatrix} \Omega_{P0} - \Omega_{H0} \\ \Phi_{P0} \end{bmatrix} \right\} \Delta\beta$$

$$\Delta Q_{PL} = \frac{\delta M_{PAL\theta}}{d\Omega_H} \Delta\Omega_H + \frac{\delta M_{PAL\theta}}{\delta V_P} \Delta V_P \tag{27}$$

The resulting linear dynamics for the power take-off are

$$J_S \Delta\dot{\Omega}_S = \Delta Q_S - \Delta T_{RG} \quad ; \quad \Delta\dot{T}_{RG} = K_S(\Delta\Omega_S - \Delta\Omega_G) \quad ; \quad J_G \Delta\dot{\Omega}_G = \Delta T_{RG} - 2k_{c0}\Omega_{S0}\Delta\Omega_S - \Omega_{G0}^2 \Delta k_c \tag{28}$$

$$\Delta Q_S = \frac{\partial Q_S}{\partial \Omega_S} \Delta\Omega_S + \frac{\partial Q_S}{\partial \Omega_P} \Delta\Omega_P \quad ; \quad \Delta T_S = \frac{\partial T_S}{\partial \Omega_S} \Delta\Omega_S + \frac{\partial T_S}{\partial \Omega_P} \Delta\Omega_P \tag{29}$$

and the linear dynamics for the simplified model for the power take-off, when the bandwidth of the power take-off is sufficiently large, are

$$\Delta Q_S = \frac{\partial Q_S}{\partial \Omega_P}\Delta\Omega_P + \frac{\partial Q_S}{\partial k_c}\Delta k_c \quad ; \quad \Delta T_S = \frac{\partial T_S}{\partial \Omega_P}\Delta\Omega_P + \frac{\partial T_S}{\partial k_c}\Delta k_c \tag{30}$$

These linear dynamics can be used to design the full envelop controller, C.

5 Illustrative examples of the linear dynamics

A MATLAB script has been generated to determine the equilibrium operating points associated with an operational strategy for a particular X-Rotor turbine. These equilibrium operating points are then input to a further MATLAB script to determine the local linear dynamics. The linear equations for the sub-systems described in Sections 4 and 5 are reformulated in state space form and linked together by the script. Linear models in state space, transfer function on Bode plot form are created and output. Some examples are provided below for 12.55m/s wind speed. The Bode plots for the transmittance from $\Delta\beta$ to $\Delta\Omega_H$ and from Δk_c to $\Delta\Omega_H$ are shown in Figures 8 and 9, respectively.

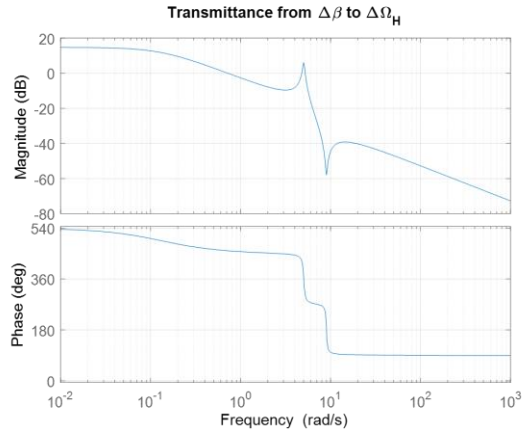

Figure 8: Bode plot for transmittance from pitch angle to cross-arm speed

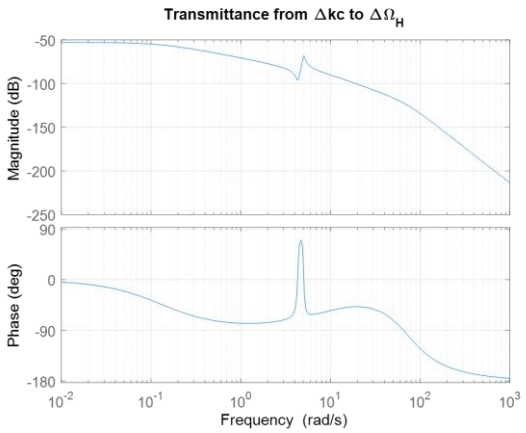

Figure 9: Bode plot for transmittance from k_c to cross-arm speed

6 Conclusions

Based on the work being undertake in Tasks 3.1 and 3.4, an overview of the X-rotor's operational strategy and the structure of the dynamics of the turbine and its controller is provided In Section 2. From this it is clear, that the inputs to the X-Rotor full envelop controller are the primary rotor speed and secondary rotor speeds or equivalently the frequencies of the power connections to the generators. The outputs are pitch angle demand for the upper primary rotor blades and a parameter that is equivalent to a tip speed ratio demand. It is, also clear that a separate controller incorporated into each power take-off unit, consisting of a secondary rotor, generator and converter, is required. These additional controllers are tasked with ensuring that the secondary rotor speed and aerodynamic torque maintain the relationship required to achieve the required tip speed ratio.

Informed by Section 2, a nonlinear dynamic model of the power take-off unit and its associated linearised model, suitable for design of the power take-off controller, are described in Section 3. In addition, a nonlinear dynamic model of the X-Rotor turbine and its associated linearised model, suitable for design of the full envelop controller, are described in Section 4. The nonlinear models in Section 3 and Section 4 are modifications of the nonlinear simulation models reported in deliverable D3.2 [4]. A MATLAB script to determine the linear models for a given X-Rotor operational strategy is developed. Some illustrative examples are provided in Section 5.

7 References

[1] Kundur, P., *Power system stability and control*, McGraw-Hill, New York, 1993

[2] Connor, B., Leithead, W. E., *Control of variable speed wind turbines: dynamic models*, Int. Journal of Control, Vol. 73, No. 13, pp1173-1188, 2000.

[3] Dudgeon, G. J. et al, *The effective role of AVR and PSS in power systems: Frequency response analysis*, *IEEE Transactions on Power Systems, 22*(4), 1986-1994, 2007

[4] Leithead, W. E., et al, *D3.2. Control simulation model of X-Rotor concept*, March 2022

[5] Leithead, W. et al, *The X-Rotor Offshore Wind Turbine Concept*, Journal of Physics: Conference Series, *1356*(1), 0-10, 2019.

[6] Leithead, W., Rogers, M., (1996). *Drive-train Characteristics of Constant Speed HAWT's: Part I-Representation by Simple Dynamic Models Part I*. Wind Engineering, 20(3), 1996